



Published in final edited form as:

Biomacromolecules. 2024 March 11; 25(3): 1800–1809. doi:10.1021/acs.biomac.3c01258.

Decreased Lung Metastasis in Triple Negative Breast Cancer Following Locally-Delivered Supratherapeutic Paclitaxel-Loaded Polyglycerol Carbonate Nanoparticle Therapy

Robert C. Sabatelle, PhD^{1,T}, Ngoc-Quynh Chu, MD^{2,3,T}, William Blessing, PhD³, Hussein Kharroubi, MD³, Eric Bressler¹, Lillian Tsai, MD², Angela Shih, MD⁴, Mark W. Grinstaff, PhD^{1,*}, Yolonda Colson, MD PhD^{2,3,*}

¹Boston University, Departments of Chemistry and Biomedical Engineering, Boston, MA 02215

²Beth Israel Deaconess Medical Center, Department of Surgery, Boston, MA 02215

³Massachusetts General Hospital, Department of Surgery, Boston, MA 02114

⁴Massachusetts General Hospital, Department of Pathology, Boston, MA 02114

Abstract

Breast cancer is among the most prevalent malignancies, accounting for 685,000 deaths worldwide in 2020, largely due to its high metastatic potential. Depending on stage and tumor characteristics, treatment involves surgery, chemotherapy, targeted biologics, and/or radiation therapy. However current treatments are insufficient for treating or preventing metastatic disease. Herein, we describe supratherapeutic paclitaxel-loaded nanoparticles (81 wt% paclitaxel) to treat the primary tumor and reduce the risk of subsequent metastatic lesions in the lungs. Primary tumor volume and lung metastasis reduce by day 30 compared to the paclitaxel clinical standard treatment. The ultra-high levels of paclitaxel afford an immunotherapeutic effect, increasing natural killer cell activation and decreasing NETosis in the lung, which limits the formation of metastatic lesions within the lung.

Graphical Abstract

*Corresponding Authors: Yolonda L. Colson, MD, PhD, 55 Fruit Street, Boston, MA 02114, ycolson@mgh.harvard.edu, Mark W. Grinstaff, PhD, 590 Commonwealth Avenue, Boston, MA 02215, mgrin@bu.edu.

^TCo-First authors: Drs. Sabatelle and Chu

Author Contributions

Conceptualization: RCS, NQC, WAB, MWG, YLC

Methodology: RCS, NQC, WAB, HK, EB, LLT, ARS

Investigation: RCS, NQC, WAB, HK, EB, LLT, ARS

Visualization: RCS, NQC

Supervision: MWG, YLC

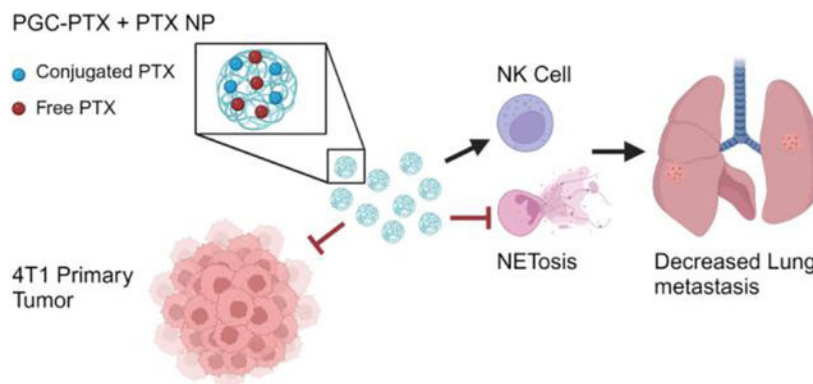
Writing—original draft: RCS, NQC, WAB

Writing—review & editing: All authors

Funding: MWG, YLC

Competing interests

RSB, YLC, and MWG are co-inventors on a patent application, which is available for licensing. All other authors declare they have no competing interests.



Created with [BioRender.com](https://www.biorender.com)

Keywords

breast cancer; metastatic lesions; nanoparticles; immunotherapy; supratherapeutic; paclitaxel

Introduction

Breast cancer is the world's most prevalent cancer¹. Globally, more than 2 million new cases of invasive breast cancer will be diagnosed in 2023, with about 298,000 cases in the United States, as estimated by The American Cancer Society and the National Cancer Institute Surveillance, Epidemiology, and End Results Program^{2,3}. Breast cancer is characterized by a description of the cancer's histopathology, tumor grade, tumor stage, and receptor status – these characteristics inform prognosis and guide treatment modalities and options. Receptor status is a critical assessment as it determines the effectiveness of available targeted treatments. There are three receptor-based subtypes on which targeted therapy is based: a) hormone receptor estrogen (ER) or progesterone (PR) positive, b) receptor tyrosine-protein kinase erbB-2 [ERBB2 or also referred to as HER-2] positive, or c) triple negative, characterized by the lack of expression of molecular targets ER, PR, or HER-2. Triple negative breast cancer (TNBC) has a higher risk of distant relapse in the first 3 to 5 years following diagnosis⁴ and carries a significantly worse 5-year survival rate owing to a 4-fold higher probability of metastasis⁵. Patients who develop distant metastases demonstrate significantly worse 5-year survival compared to patients in which the primary breast cancer remains localized or only spreads to regional lymph nodes (23.4% vs 98.6% and 83.8%, respectively)⁶. Given the poor 5-year survival associated with metastatic breast cancer and TNBC, there is a critical need for novel treatment approaches to prevent distant tumor spread.

Treatment of early-stage non-metastatic breast cancer is primarily surgical resection with lymph node dissection in addition to adjuvant or neoadjuvant systemic/hormonal therapy⁷. However, locoregional treatment in breast cancer patients with evidence of metastasis at presentation does not have a survival benefit⁸. Kobayashi et al. report improved outcomes in patients receiving local therapies with increasing overall survival rates of 82% and 53% at 10 and 20 years, respectively. However, outcomes worsen for patients with metastatic

lesions due to poor existing treatment options^{9,10}. For patients treated with chemotherapy, only 1–2% of the patients diagnosed with metastatic cancer are long-term disease-free survivors, with outcomes closely tied to the extent of metastases^{11–13}. Furthermore, micro-metastatic disease may not be detectable. These clinical data highlight a lack of treatments for metastatic TNBC, as well as the urgency for investigating novel treatments in preclinical studies. A local, highly effective chemotherapy regimen that treats both local tumor and distant metastases would significantly enhance patient care and decrease mortality percentages.

Paclitaxel (PTX) is a first-line chemotherapy as a single-agent drug or in combination with monoclonal antibody drugs to treat breast cancer. However, systemic administration precludes high concentrations from accumulating within the tumor and lymphatics due to poor pharmacokinetics and significant toxicity with high systemic doses¹⁴. Treatment for HER2 positive metastatic breast cancer using a combination of two anti-HER2 receptor monoclonal antibodies (pertuzumab + trastuzumab) in addition to a taxane chemotherapeutic agent demonstrates an overall survival benefit and a median progression-free survival of 18 months¹⁵. Treatment of TNBC is much less effective, with taxane treatment resulting in only a 36% response rate and a 4.5-month progression-free survival¹⁶. Although combination chemotherapy in patients with metastatic breast cancer provides a survival advantage over single agent taxane chemotherapy, it is associated with greater toxicity¹⁷.

To bypass off-target toxicities and limited dosing of systemic chemotherapy, we imagined a system in which paclitaxel is delivered at high doses locally. As a result, we fabricated ultra-high drug loaded nanoparticles (PGC-PTX + PTX NPs) composed of poly(1,2-glycerol carbonate)-graft-succinic acid-paclitaxel (PGC-PTX) conjugate. We selected the biocompatible and biodegradable PGC for NP formation as it is as it degrades into glycerol and carbon dioxide, and it can be conjugated with chemotherapeutics. We previously demonstrated that PGC-PTX + PTX NPs are cytotoxic, have a sustained release of PTX, and are efficacious in a murine model of a non-metastatic human peritoneal mesothelioma, as compared to standard PTX dosing¹⁸. Given these encouraging results, we evaluated the efficacy of these NPs in an aggressive, immunocompetent model of murine TNBC (4T1), and propose a mechanism of action of reduced metastasis to the lungs. Administration of PGC-PTX+PTX NPs locally controls the primary tumor and decreases incidence of metastatic disease. Finally, we discuss these results in the context of current treatments in the clinic and local chemotherapy as well as other nanoparticle formulations under investigation.

Materials and Methods

PGC-PTX Synthesis

Poly(1,2-glycerol carbonate)-graft-succinic acid-paclitaxel with 39 mol% paclitaxel conjugation (PGC-PTX; Figure 1A) and PGC-PTX with 10 mol% rhodamine B conjugation (PGC-PTX-Rho) were synthesized^{18,19}. Briefly, poly(benzyl 1,2-glycerol carbonate) (PGC-OBn) was synthesized via copolymerization of benzyl glycidyl ether and carbon dioxide. The benzyl group was deprotected via high pressure hydrogenolysis to yield poly(1,2-glycerol carbonate) (PGC). PGC was subsequently reacted with succinic anhydride and 4-dimethylaminopyridine (DMAP) in dimethylformamide (DMF) to obtain poly(1,2-glycerol

carbonate)-graft-succinic acid, which possesses a free carboxylic acid group on each repeating unit. PTX was conjugated using N,N'-dicyclohexylcarbodiimide (DCC) and DMAP in DMF to afford PGC-PTX (70% yield). The polymer molecular weight was determined via gel permeation chromatography and found to be 14,800 g/mol with a PDI of 1.04. NMR analysis provided the amount of PTX conjugated to the polymer. Rhodamine-conjugated PGC-PTX was synthesized by first reacting PGC with rhodamine B isothiocyanate for four hours, then subsequent conjugation of succinic acid and PTX using the procedure above. Rhodamine B conjugation to the polymer was confirmed by NMR and fluorescence.

Preparation of Polyglycerol Carbonate Nanoparticles

NPs were prepared by miniemulsion as previously described²⁰. Briefly, free PTX was added to 50 mg of PGC-PTX (58wt% PTX) polymer to give a mixture containing 25wt% free PTX. PGC-PTX and PTX were then dissolved in 0.5 mL dichloromethane, and added to a 2 mL solution of sodium dodecyl sulfate (SDS) in pH 7.4, 10 mM phosphate buffer at a 1:5 SDS:polymer mass ratio. The mixture was emulsified under an argon blanket using a Sonics Vibra-Cell VCX-600 Ultrasonic Processor (Sonics & Materials; Newtown, CT). Following sonication, the NP suspension was stirred under argon for 2 h, followed by stirring under air overnight to allow for the evaporation of remaining organic solvent. The resulting NP suspension was dialyzed for 24 hours against 1 L of 5 mM pH 7.4 phosphate buffer. The dialysis buffer was exchanged with fresh buffer after 10 hours of dialysis. The free PTX encapsulation efficiency is 90+% by HPLC. Total drug loading was also quantified via HPLC analysis and is defined as the mass of the drug divided by the mass of the carrier. The final drug loading for this PGC-PTX + PTX formulation is ~81 wt%, due to the combination of free PTX (23 wt%) and conjugated PTX (58 wt%).

Drug-free PGC-OBn NPs and PGC-PTX NPs were also prepared using the same procedure. Particle size and zeta potential were measured by DLS, resulting in diameters of ~80 nm, PDI of ~0.1, and -40 mV zeta potentials for all three NP formulations. Size and charge were independent of drug/fluorophore loading. Scanning electron microscopy confirmed spherical NPs (Figure 1B). *In vitro* PTX release from the PGC-PTX + PTX NP occurred over 60 days, as previously described²¹. Over the last five years, four different graduate students have prepared these NPs indicating that the NP fabrication process is reproducible.

Cell Culture and Maintenance

4T1 cells were purchased from ATCC (Manassas, VA) and were cultured in accordance with vendor protocol. Briefly, 4T1 cells were grown on cell culture-treated tissue culture plates and grown in RPMI 1640 with 10% fetal bovine serum and 1% penicillin/streptomycin in a humidified incubator maintained at 37 °C and 5% CO₂. Cells were subcultured at 70–90% confluency or at vendor-recommended density.

Establishment of 4T1 Orthotopic *in vivo* Murine Model

Five- to seven-week-old female Balb/c mice were purchased from Jackson Laboratories (Bar Harbor, ME). Under inhaled anesthesia and sterile prep, the 4th mammary fat pad was exposed via a very small cutdown incision overlying the fat pad. A 100 µL suspension

of 100,000 4T1 cells in phosphate-buffered saline was injected directly into the mammary fat pad and the incision closed with a wound clip. Tumor establishment was confirmed by palpation of a small nodule (usually around day 7 post-implant).

Treatment of Established Tumor

One week after tumor inoculation, animals received 30 μ L of one of the following “treatments” injected subcutaneously near the tumor: saline (n=9), 100 mg/kg PTX as PGC-PTX+PTX NPs (n=14), or polymer mass-equivalent non-drug-loaded PGC-OBn NPs (n=10). Standard PTX treatment controls received weekly doses of intraperitoneal (IP) 20 mg/kg PTX-C/E (n=8) for three weeks to afford systemic delivery of PTX at the maximum allowable (20mg/kg single maximum tolerated dose for PTX-C/E). PGC-PTX+PTX NPs are safely delivered at a higher dose, as we previously established.¹⁸

Tumor burden was analyzed via tumor volume measurements calculated with the following formula: $\frac{\pi}{6} * length * width * height$. All animals were monitored 3x per week and were euthanized at the predetermined endpoint of 30 days or upon evidence of cachexia or moribund status per Institutional Animal Care and Use Committee guidelines. At the time of euthanasia, primary tumor, lungs, lymph nodes, spleen, liver, and heart were harvested for postmortem and/or histological analysis.

Analysis of Pulmonary Metastatic Lesions

Metastatic nodules on the lung were counted following a published protocol²². Briefly, a solution of 10% India ink in phosphate-buffered saline was prepared. The mouse chest was opened and a suture was tightly tied around the top of the trachea. Up to 1 mL of India ink solution was infused directly into trachea until both lungs were fully saturated with ink. Stained lungs were harvested, fixed, and destained in Feteke’s solution. Metastatic nodules on each lung were counted.

Histological Analysis

Harvested tissue specimens were either immediately embedded in OCT, flash frozen in a liquid nitrogen/isopentane bath, and stored in -80 °C; or fixed overnight in 10% phosphate-buffered formalin before submission to the Massachusetts General Hospital Histopathology core. Tissues were mounted onto glass slides as 4 μ m cross sections before downstream immunohistochemistry, immunofluorescence, or H&E staining. All histological analyses were confirmed with pathologist consultation.

Immunofluorescence / Fluorescence Microscopy and Confocal Laser Microscopy

Paraffin-embedded sections were de-paraffinized and rehydrated by 15 minute incubation at 60 °C followed by 3 minute incubations in the following solutions: xylene x 2, 1:1 xylene:ethanol (etOH), etOH x 2, 95% etOH, 70% etOH, 50% etOH, 25% etOH, distilled water x 2. Slides were then incubated in 1X Immunofluorescence Wash Buffer (Cell Signaling Technologies, Danvers, MA) for 5 minutes. Tissue sections were blocked using 1X Immunofluorescence Blocking buffer (Cell Signaling Technologies) for 1–2 hours at room temperature. Primary antibodies were diluted in 1X Antibody Dilution Buffer (Cell

Signaling Technologies), and tissues were incubated in primary antibody overnight at 4 °C. Specimens were washed 3x in PBS for 5 minutes each. Secondary antibody was prepared the same way as primary, and tissues were incubated in secondary for 1–2 hrs at room temperature, protected from light. Samples were washed as before prior to DAPI and/or WGA-AlexaFluor counterstaining and mounting with Prolong Gold Antifade (Thermo Fisher Scientific, Waltham, MA). Fluorescent imaging was performed in the Microscopy Core.

Flow Cytometry and NP Uptake Quantification

4T1 cells were plated at 3×10^5 cells/mL in 6-well plates and co-incubated with rhodamine B-labeled NPs at 200ng/mL for 0–24 hours as indicated. Cells were then lifted from the plate via trypsinization, washed twice via centrifugation for 5 minutes to remove residual NPs, and strained to obtain a single cell suspension. NP uptake was then quantified on the Attune NxT Flow Cytometer (ThermoFisher Scientific) and data was analyzed in FlowJo X.

Results

Synthesis of the PGC-PTX + PTX NPs.

We first synthesized the pre-cursor polymer, poly(benzyl 1,2-glycerol carbonate) (PGC-OBn), using a cobalt-catalyzed copolymerization of benzyl glycidyl ether and carbon dioxide. Next, we removed the benzyl group via high pressure hydrogenolysis to yield poly(1,2-glycerol carbonate) (PGC) which was then subsequently reacted with succinic anhydride and DMAP to obtain poly(1,2-glycerol carbonate)-graft-succinic acid. A DCC based esterification with PTX yielded the PGC-PTX. By varying the amount of PTX added, drug loadings ranging from 10 to 70 wt% were achievable due to the small molecular weight of the repeating unit in the PGC backbone. For all subsequent studies, we used poly(1,2-glycerol carbonate)-graft-succinic acid-paclitaxel with 39 mol% paclitaxel conjugation as determined by NMR spectroscopy (Figure 1A).

We prepared NPs using a reproducible miniemulsion procedure,²⁰ where free PTX was added to 50 mg of PGC-PTX (58wt% PTX) polymer in 0.5 mL of dichloromethane to a mixture containing 25wt% free PTX. We then sonicated the dichloromethane solution in the presence of a 2 mL solution of sodium dodecyl sulfate (SDS) in pH 7.4, 10 mM phosphate buffer at a 1:5 SDS:polymer mass ratio. To remove the excess SDS, the NPs are dialyzed for 24 hours. The SDS present coats the exterior of the NP enhancing stability while also being low enough in concentration to not cause toxicity.²⁰ After work-up and dialysis, we determined the PTX loading of the PGC-PTX + PTX formulation to be ~81 wt%, as a consequence of free PTX (23 wt%) and conjugated PTX (58 wt%). The NPs are ~80 nm in diameter, with a PDI of ~0.1, and possess a zeta potential of –40 mV by DLS and spherical in shape by SEM (Figure 1B). In a previous study, we reported that the PGC-PTX + PTX NPs are stable both in solution at 4 °C and lyophilized at –20 °C over seven weeks.¹⁸

In Vitro Characterization of the PGC-PTX + PTX NPs on 4T1 Tumor Cells

We determined the cytotoxicity of PGC-PTX + PTX NPs *in vitro*. The NPs are cytotoxic against 4T1 cells (IC50 of 87.75 ng/mL), as well as other breast cancer lines including

MDA-MB-231 (20.82 ng/mL) and MCF-7 (4.67 ng/mL) after a 3-day exposure (Figure 1C). The PGC-PTX + PTX NPs display a similar cytotoxicity profile to clinical paclitaxel formulations (PTX-C/E), while the nanocarrier itself is non-toxic (Figure S1). PGC-PTX + PTX NPs are similarly cytotoxic to human mesothelioma cancer cell lines (MSTO-211H, H266, H2453, and H28)²¹ suggesting that they may be applicable to other cancers. To determine the cellular uptake of PGC-PTX+PTX NP, we covalently conjugated rhodamine-B (Rho) to the polymer (PGC-PTX) prior to emulsification to synthesize PGC-PTX-Rho + PTX NPs. As shown in Figure 1D, uptake of these fluorescently-tagged NPs by tumor cells saturates after 6 hours, indicating rapid internalization. The cytotoxic effect of these NPs is tied to two factors: high PTX encapsulation and rapid NP uptake. The PTX conjugated to the polymer backbone hydrolyzes and is released over the span of two months²¹ while encapsulated PTX releases over weeks.²⁰

Locally Administered Paclitaxel-Loaded Nanoparticles Inhibit Tumor Growth

To demonstrate the impact of local treatment and the efficacy of PGC-PTX + PTX NPs *in vivo*, we evaluated the NPs against an orthotopic metastatic breast cancer model. The 4T1 metastatic breast cancer mouse model is a well characterized and aggressive tumor model with consistent tumor uptake after implantation and metastasis to the lung. One week after tumor inoculation, we randomly selected mice for one of four treatment groups: subcutaneous/peritumoral injections of saline, unloaded nanoparticles (PGC-OBn), PGC-PTX +PTX NPs, or systemic intraperitoneal (IP) paclitaxel (PTX-C/E). For the PTX-C/E group, three doses total were delivered at 1-week intervals (Figure 2A). Compared to PGC-OBn and saline controls, which are statistically indistinguishable, local administration of PGC-PTX+PTX NPs significantly reduce local tumor burden as measured by growth of primary tumor volume compared to IP PTX-C/E or control groups ($p < 0.01$) (Figure 2B). Likewise, tumor weights at day 30 are significantly lower for PGC-PTX+PTX NP-treated animals ($p < 0.0001$) as compared to either saline, unloaded control NPs, or IP PTX-C/E treated controls, which are not statistically different from each other (Figure 2C). Over the planned 30 days of observation, all mice maintain body weights within 20% of the initial body weight prior to 4T1 inoculation (Figure S2). Histological analysis of tumor in each treatment group reveals that saline, PGC-OBn NPs and IP PTX-C/E treatments afford tumors with large areas of viable tumor, whereas the PGC-PTX+PTX NP-treated tumors are necrotic with sparse population of viable tumor cells, as indicated by the irregular nuclei (Figure 2D). Notably, tumors treated with the PGC-PTX + PTX NPs show significant regions of fat tissue akin to the histological hallmarks of healthy, tumor-free breast tissue. We also analyzed the ipsilateral axillary lymph nodes of the treated mice after tumor inoculation and observed no significant difference in lymph metastasis between treatment groups.

Biodistribution of Locally-Administered PGC-PTX + PTX Nanoparticles

Following the same treatment schedule as previously noted, we treated 4T1 tumor-bearing mice with PGC-PTX-Rho + PTX NPs to investigate the biodistribution of locally, subcutaneously administered NPs near the tumor. Over a 30-day period, NP accumulation in the tumor appears greatest at day 15 and reduces by day 30. NPs are present at the periphery as well as within the tumor.. Interestingly, rhodamine-labelled nanoparticles do

not reach the lungs by day 8, yet there is rhodamine signal on day 30 (Figure 3). At day 30, NPs accumulate at the edge of the lung. One possible migration route consistent with this observation is lymphatic drainage from the tumor or subcutaneous injection site.

High Dose PTX Modulates Immunity to Reduce Lung Metastasis

Consistent with prior reports on the orthotopic 4T1 murine breast cancer model, we observed a consistent and significant rate of lung metastasis^{23,24}. With PGC-PTX + PTX NPs treatment, there is a marked reduction in the number of pulmonary metastatic lesions as compared to the saline and IP PTX-C/E controls ($p < 0.01$, $p < 0.05$, respectively; Figure 4A). As shown in figure 4B, the India ink-stained lungs exhibit a lower number of metastatic lesions as compared to the other groups.

Histological Analysis of Ultra High PTX Dosage on Tumor Metastasis

To further understand the mechanism by which the PGC-PTX +PTX NPs reduce metastasis to the lungs, we performed immunohistological analysis of the lung tissues on day 30 to assess the microenvironment. Figure 5A details one pathway in which 4T1 tumor cells migrate and establish metastatic foci within the lungs as reported in the literature^{25,26}. Immunohistochemical staining for citrullinated peptide H3 (citH3), which is a specific marker for neutrophil extracellular traps (NETs) formation, is present in the lungs of mice treated with saline controls. Similarly, although decreased in the lungs of mice treated with systemic PTX-C/E given IP, NETosis is still prevalent, consistent with the subsequent high number of lung metastases that develop in these animals (Figure 5B, panel 2). In contrast, animals treated with PGC-PTX+PTX NPs show no citrullinated peptide H3 staining, indicating no significant NETosis occurring in the lungs of these NP treated animals. Similarly, mice treated with PGC-PTX+PTX NPs exhibit an increase in activated natural-killer cells (NK1.1+, CD107a+, IFN γ +) in the lungs (Figure 5C), congruent with the observation of markedly decreased numbers of metastatic lesions. These results suggest that effective local treatment prevents metastatic niche formation by decreasing NETosis and increasing NK activity thereby decreasing the number of circulating tumor cells. This is a potential new role for PTX which becomes significant at high concentrations.

Discussion

Low five-year survival rates for patients with metastatic breast cancer can be attributed to difficulty in effectively treating the primary tumor and preventing distant metastases²⁷. Current treatment options include surgery, local radiation, systemic chemotherapy, and targeted therapies. These treatments are effective for early-stage, receptor positive breast cancer but less so for TNBC, which has an increased incidence of metastases, and a significantly decreased survival rate. Specifically, patients with HER2+ breast cancer benefit from the addition of anti-HER2 receptor therapies such as trastuzumab, pertuzumab and neratinib to a chemotherapeutic regimen that includes taxanes²⁸. On the other hand, TNBC lacks targetable surface markers, and therefore treatment of TNBC depends mainly on a chemotherapeutic regimen that includes taxanes and platinum-based compounds²⁹. The absence of surface receptor expression has led to the search for new therapeutic options³⁰. Capecitabine, when added to adjuvant chemotherapy, prolongs disease free and

overall survival in triple negative breast cancer patients as compared to standard therapy³¹. There is also emerging evidence that the addition of immunotherapy, such as PD1/PD-L1 inhibitors, to the treatment regimen may benefit patients with early stage or advanced triple negative breast cancer³². For example, the addition of pembrolizumab to other neoadjuvant chemotherapy in patients with stage II-III TNBC, as reported in the KEYNOTE-522 clinical trial, results in a higher pathologic complete response at the time of surgery and reduced disease progression and recurrence as compared to patients who do not receive pembrolizumab over a median follow up period of 15.5 months²⁹.

In addition to novel therapeutic targets, alternative methods of drug delivery to improve the efficacy of existing cancer drugs should also be explored. Local drug delivery is as an alternate strategy to achieve high local chemotherapy concentrations at the site of tumor to prevent local recurrence while minimizing off-target toxicities and dose-limiting systemic delivery effects^{33,34}. Hydrogels are a common local delivery platform due to their ability to trap and release chemotherapeutics at the tumor site. For example, delivery of a self-healing doxorubicin (DOX) loaded hydrogel, when combined with near-infrared phototherapy (NIR), reduces recurrence in a murine 4T1 model compared to their controls. However, due to a burst release of DOX (50% released in under 10 hours), this treatment is not nearly as efficacious without the NIR phototherapy³⁵. The poor pharmacokinetics associated with hydrogels can be superseded using a nanoparticle-aggregated hydrogel. As the aggregate degrades, tumor-targeting NPs loaded with DOX release and enter the surrounding tumor cells. This formulation affords DOX release over the span of weeks. When tested in a murine breast cancer model, survival minimally improves compared to intravenous DOX controls³⁶.

Nanoparticles are widely implemented in experiments for local chemotherapy due to their tunability and flexibility as a drug delivery platform. In fact, treatment of TNBC with albumin-bound paclitaxel (Nab paclitaxel) has gained attention and is being investigated in clinical trials^{37,38}. Nanoparticle formulations allow for encapsulation of several drugs for combination therapy^{39,40}, improve drug biodistribution⁴¹, and salvage the tumor's intrinsic characteristics to deliver the payload⁴². One such example is Da Rocha et al.'s solid-lipid nanoparticles loaded with docetaxel. These nanoparticles demonstrate an anti-tumor effect in a similar 4T1 murine model of metastatic breast cancer while also significantly decrease lung metastasis by decreasing IL-6 secretion. However, 5 injections are required over the span of 20 days, likely due to the relatively quick release of drug (~50% in 5 days), and low drug loadings (2%)⁴³. Employing well-established PLGA nanoparticles, Anasamy et al. locally delivered several novel tribenzyltin carboxylates to evaluate their cytotoxicity and anti-tumor effect. Two administrations of these nanoparticles a week apart significantly reduce the primary tumor, and additionally prevent metastasis in the lungs and liver 15-days after inoculation⁴⁴. These publications demonstrate tumor suppression and short-term prevention of metastasis *in vivo*, and provide the impetus for further study. Today, there is a need for novel, local breast cancer treatments that limit metastasis while decreasing primary tumor burden long-term.

The 4T1 breast cancer model was developed in the 1990s⁴⁵⁻⁴⁷, and it remains one of the most rigorous immunocompetent murine models of TNBC⁴⁸⁻⁵⁰. 4T1 tumor cells secrete

high amounts of chemokines that lead to the expansion and activation of the neutrophil population in the spleen leading to splenomegaly and neutrophilia. Neutrophils play an important role, as reported by Spiegel et. al., in the establishment of lung metastatic lesions in the 4T1 model. Neutrophils inhibit NK cell activation thereby decreasing clearance of disseminated circulating cancer cells within the pulmonary microvasculature. Neutrophils also facilitate the extravasation of these cells at the lungs⁵¹. Additionally, neutrophils undergo a process known as NETosis, which involves the release of chromatin and protein bound complexes called Neutrophil Extracellular Traps (NETs). Though traditionally used by neutrophils in clearing pathogens, NETosis in the context of cancer creates a metastatic niche. The modification of histone H3 by citrullination via a calcium-dependent mechanism involving PAD4 enzyme is a hallmark of NET formation and is a specific marker for NETosis *in vivo*⁵². Therefore, we investigated NETosis and NK cell activity in tumor bearing animals as a potential mechanism for decreased lung metastasis observed with treatment with our PGC-PTX+PTX NPs.

4T1 breast cancer tumor cells afford a significant boost of NET formation in the lungs of our animals, similar to previously reported studies in the literature^{53–55}. However, local treatment of PGC-PTX + PTX NPs results in significantly lower primary tumor volume by day 30 due as well as fewer metastatic lesions in the lung, increased NK cell activation, and decreased NETosis in the lungs. We propose this result is a consequence of the high PTX concentration in the NP formulation and extended release,²⁰ compared to PTX alone which is cleared from circulation within hours. The loss of NETs in the lungs likely eliminates the niche required for circulating tumor cells to implant, contributing to the reduction of metastatic lesions^{56–58}. Similar to the inhibition of NETosis, treatment of the primary tumor via PGC-PTX+PTX NPs also increases the number of activated natural killer cells within the lungs. Natural killer cells are one of the main contributors to decreasing circulating tumor cells and thus prevent lung metastases⁵⁹, although they can be inhibited by neutrophils due to their generation of reactive oxygen species^{60–62}. It is of note that although NETosis decreases and NK cell activation increases within the lungs, the PGC-PTX+ PTX NPs themselves make their way to the lungs by day 30, potentially contributing to decreased metastasis by direct drug toxicity as well.

The immunomodulatory role of nanoparticle albumin-bound paclitaxel (Nab-paclitaxel) in promoting anti-tumor immunity by overcoming an immunosuppressive microenvironment has been reported in the literature⁶³. Our PGC-PTX + PTX NPs are effective not only in treating the primary tumor but also in inducing an anti-metastatic immune profile in the lung that is capable of preventing the establishment of metastatic disease. These results suggest that there is a potential immunomodulatory impact of local, highly concentrated levels of PTX. Future work includes investigation of the specific cytokine response after ultra-high levels of PTX in the tumor bed, as well as a deeper investigation into immune cell activation in surrounding lymph nodes and organs. Specifically, chemotherapies are reliant on their ability to induce immunogenic cell death, which relies on damage-associated molecular patterns (DAMPs) from dying cells. Work done by Lau et al.⁶⁴ and Sprooten et al.⁶⁵ demonstrate that paclitaxel's efficacy is linked to DAMPs, and this pathway will be evaluated in future studies after PGC-PTX + PTX treatment. This knowledge will be leveraged to supplement the anti-tumor efficacy of paclitaxel to inform the development of

an effective treatment that targets both primary tumor and distant metastases, while limiting off-target toxicities.

Conclusion

In summary, local delivery and sustained release of high paclitaxel concentrations suppresses tumor growth and reduces lung metastasis via decreasing NETosis and increasing natural killer cell activation. In this murine model of lung metastasis, we demonstrate that the rapid cellular uptake of the PGC-PTX+PTX NPs, coupled with their ultra-high paclitaxel loading, imparts a highly cytotoxic effect on several breast cancer cell lines *in vitro*. *In vivo*, local s.c injections of the PGC-PTX+PTX NPs significantly reduce primary tumor growth compared to the maximally tolerated PTX-C/E control systemically administered in an orthotopic murine model. Notably, local NP treatment affords a significant decrease in lung metastasis due to immunomodulatory effects, resulting in a decrease in NETosis, an increase in activated natural killer cells in the lungs, and presumably fewer metastatic niches. This understanding of local chemotherapy and its impact on breast cancer metastasis provides important information and supports further development of this technology or similar ones that are both cytotoxic and immunomodulatory.

Supplementary Material

Refer to Web version on PubMed Central for supplementary material.

Acknowledgements

We acknowledge and thank the National Institutes of Health and the Thoracic Surgery Foundation Resident Research Award for support of this work.

Funding

Funding in part for this work was from the National Institutes of Health (R01CA 227433, MWG, YLC; R01CA232056, MWG, YLC; T32EB006359, RBS; T32GM130546, EMB; F30CA257566, EMB; DK043351 - Program in Membrane Biology Centre for the Study of Inflammatory Bowel Disease Grant; DK057521 - Boston Area Diabetes and Endocrinology Research Center (BADERC) Award, and 1S10OD021577-01 - Zeiss confocal system), and the Thoracic Surgery Foundation Resident Research Award (NQC).

Availability of data and materials

The raw data required to reproduce these findings are available from the authors upon request.

References

1. DeSantis CE et al. International variation in female breast cancer incidence and mortality rates. *Cancer Epidemiology Biomarkers and Prevention* 2015, 24, 1495–1506.
2. Siegel RL, Miller KD, Wagle NS & Jemal A Cancer statistics, 2023. *CA Cancer J Clin* 2023, 73, 17–48(). [PubMed: 36633525]
3. NCI. Cancer Stat Facts: Female Breast Cancer. 2023. date of access November 15, 2023. <https://seer.cancer.gov/statfacts/>
4. Foulkes WD, Smith IE & Reis-filho JS Triple-Negative Breast Cancer. *New England Journal of Medicine* 2010, 363, 1938–1948. [PubMed: 21067385]

5. Waks AG & Winer EP Breast Cancer Treatment: A Review. JAMA – Journal of the American Medical Association 2019, 321, 288–300. [PubMed: 30667505]
6. Redig AJ & Mcallister SS Breast cancer as a systemic disease: A view of metastasis. J Intern Med 2013, 274, 113–126. [PubMed: 23844915]
7. Waks AG & Winer EP Breast Cancer Treatment: A Review. JAMA - Journal of the American Medical Association 2019, 321, 288–300. [PubMed: 30667505]
8. Badwe R et al. Locoregional treatment versus no treatment of the primary tumour in metastatic breast cancer: An open-label randomised controlled trial. Lancet Oncol 2015, 16, 1380–1388. [PubMed: 26363985]
9. Kobayashi T et al. Possible clinical cure of metastatic breast cancer: Lessons from our 30-year experience with oligometastatic breast cancer patients and literature review. Breast Cancer 2012, 19, 218–237. [PubMed: 22532161]
10. Lebert JM, Lester R, Powell E, Seal M & McCarthy J Advances in the systemic treatment of triple-negative breast cancer. Current Oncology 2018, 25, S142–S150. [PubMed: 29910657]
11. Sledge GW Curing metastatic breast cancer. J Oncol Pract 2016, 12, 6–10. [PubMed: 26759458]
12. Greenberg PA et al. Long-term follow-up of patients with complete remission following combination chemotherapy for metastatic breast cancer. Journal of Clinical Oncology 1996, 14, 2197–2205. [PubMed: 8708708]
13. Tevaarwerk AJ et al. Survival in Metastatic Recurrent Breast Cancer after Adjuvant Chemotherapy: Little Evidence for Improvement Over the Past Three Decades. Cancer 2014, 119, 1140–1148.
14. Sparreboom A et al. Cancer Therapy : Clinical Comparative Preclinical and Clinical Pharmacokinetics of a (ABI-007) and Paclitaxel Formulated in Cremophor (Taxol). 2005, 11, 4136–4143.
15. Baselga J et al. Pertuzumab plus Trastuzumab plus Docetaxel for Metastatic Breast Cancer (CLEOPATRA). New England Journal of Medicine 2012, 366, 109–119. [PubMed: 22149875]
16. Tutt A et al. Carboplatin in BRCA1/2-mutated and triple-negative breast cancer BRCAness subgroups: The TNT Trial. Nat Med 2018, 24, 628–637. April 30, 2018 [PubMed: 29713086]
17. Carrick S et al. Single agent versus combination chemotherapy for metastatic breast cancer. Cochrane Database of Systematic Reviews 2009, 2, CD003372. doi:10.1002/14651858.CD003372.pub3.
18. Sabatelle RC et al. Ultra-high drug loading improves nanoparticle efficacy against peritoneal mesothelioma. Biomaterials 2022, 285, 121534.
19. Zhang H, Grinstaff MW. Synthesis of atactic and isotactic poly(1,2-glycerol carbonate)s: degradable polymers for biomedical and pharmaceutical applications. J Am Chem Soc. 2013, 135, 6806–9. [PubMed: 23611027]
20. Ekladios I, Liu R, Varongchayakul N, Mejia Cruz LA, Todd DA, Zhang H, Oberlies NH, Padera RF, Colson YL, Grinstaff MW. Reinforcement of polymeric nanoassemblies for ultra-high drug loadings, modulation of stiffness and release kinetics, and sustained therapeutic efficacy. Nanoscale. 2018, 10, 8360–8366. [PubMed: 29717728]
21. Ekladios I, Liu R, Zhang H, Foil DH, Todd DA, Graf TN, Padera RF, Oberlies NH, Colson YL, Grinstaff MW. Synthesis of poly(1,2-glycerol carbonate)-paclitaxel conjugates and their utility as a single high-dose replacement for multi-dose treatment regimens in peritoneal cancer. Chem Sci. 2017, 8, 8443–8450. [PubMed: 29619192]
22. Thies KA, Knoblaugh SE & Sizemore ST Pathological analysis of lung metastasis following lateral tail-vein injection of tumor cells. Journal of Visualized Experiments 2020, 159, 1–10.
23. Yang S, Zhang JJ & Huang XY Mouse models for tumor metastasis. Methods in Molecular Biology 2012, 928, 221–228. [PubMed: 22956145]
24. Pulaski BA & Ostrand-Rosenberg S Mouse 4T1 Breast Tumor Model. Curr Protoc Immunol 2000, 39, 1–16.
25. Spiegel A et al. Neutrophils suppress intraluminal NK cell-mediated tumor cell clearance and enhance extravasation of disseminated carcinoma cells. Cancer Discov 2016, 6, 630–649. [PubMed: 27072748]
26. Park J et al. Cancer cells induce metastasis-supporting neutrophil extracellular DNA traps. Sci. Trans. Med 2016, 8, 361ra. <https://www.science.org>.

27. a. Waks AG & Winer EP Breast Cancer Treatment: A Review. *JAMA - Journal of the American Medical Association* 2019, 321, 288–300. [PubMed: 30667505]
28. b. McAndrew NP & Hurvitz SA Systemic Therapy for Early- and Late-Stage, Human Epidermal Growth Factor Receptor-2-Positive Breast Cancer. *Hematol Oncol Clin North Am* 2023, 37, 103–115. [PubMed: 36435604]
29. Schmid P et al. Pembrolizumab for Early Triple-Negative Breast Cancer. *New England Journal of Medicine* 2020, 382, 810–821. [PubMed: 32101663]
30. Szymiczek A, Lone A & Akbari MR Molecular intrinsic versus clinical subtyping in breast cancer: A comprehensive review. *Clin Genet* 2021, 99, 613–637. [PubMed: 33340095]
31. Li Z et al. Addition of Capecitabine to Adjuvant Chemotherapy May be the Most Effective Strategy for Patients With Early-Stage Triple-Negative Breast Cancer: A Network Meta-Analysis of 9 Randomized Controlled Trials. *Front Endocrinol (Lausanne)* 2022, 13, 1–11.
32. Zhang M, Song J, Yang H, Jin F & Zheng A Efficacy and safety of PD-1/PD-L1 inhibitors in triple-negative breast cancer: a systematic review and meta-analysis. *Acta Oncol (Madr)* 2022, 61, 1105–1115.
33. Wolinsky J, Colson Y & Grinstaff M Local Drug Delivery Strategies for Cancer Treatment: Gels, Nanoparticles, Polymeric Films, Rods, and Wafers. *Journal of Controlled Release* 2012, 159, 1–7. [PubMed: 22482835]
34. Bressler EM et al. Doxorubicin-Loaded Polymeric Meshes Prevent Local Recurrence After Sarcoma Resection While Avoiding Cardiotoxicity. *Cancer Res* 2022, 82, 4474–4484. [PubMed: 36169924]
35. Li Q et al. Graphene-Nanoparticle-Based Self-Healing Hydrogel in Preventing Postoperative Recurrence of Breast Cancer. *ACS Biomater Sci Eng* 2019, 5, 768–779. [PubMed: 33405838]
36. Liu H et al. Injectable, Biodegradable, Thermosensitive Nanoparticles-Aggregated Hydrogel with Tumor-Specific Targeting, Penetration, and Release for Efficient Postsurgical Prevention of Tumor Recurrence. *ACS Appl Mater Interfaces* 2019, 11, 19700–19711. [PubMed: 31070356]
37. Forero-Torres A et al. TBCRC 019: A phase II trial of nanoparticle albumin-bound paclitaxel with or without the anti-death receptor 5 monoclonal antibody tigatuzumab in patients with triple-negative breast cancer. *Clinical Cancer Research* 2015, 21, 2722–2729. [PubMed: 25779953]
38. Murphy C et al. Tailored NEOadjuvant epirubicin, cyclophosphamide and Nanoparticle Albumin-Bound paclitaxel for breast cancer: The phase II NEONAB trial—Clinical outcomes and molecular determinants of response. *PLoS One* 2019, 14, 1–20.
39. El-Sahli S et al. A triple-drug nanotherapy to target breast cancer cells, cancer stem cells, and tumor vasculature. *Cell Death Dis* 2021, 12, 8. [PubMed: 33414428]
40. Atukorale PU et al. Nanoparticle encapsulation of synergistic immune agonists enables systemic codelivery to tumor sites and IFN β -driven antitumor immunity. *Cancer Res* 2019, 79, 5394–5406. [PubMed: 31431457]
41. Chaudhuri A et al. Lipid-Based Nanoparticles as a Pivotal Delivery Approach in Triple Negative Breast Cancer (TNBC) Therapy. *Int J Mol Sci* 2022, 23, 10068. [PubMed: 36077466]
42. Liu R et al. Prevention of nodal metastases in breast cancer following the lymphatic migration of paclitaxel-loaded expansile nanoparticles. *Biomaterials* 2013, 34, 1810–1819. [PubMed: 23228419]
43. da Rocha MCO et al. Docetaxel - loaded solid lipid nanoparticles prevent tumor growth and lung metastasis of 4T1 murine mammary carcinoma cells. *Journal of Nanobiotechnology*, 2020, 18, 1–20. [PubMed: 31898555]
44. Anasamy T, Fei C, Voon L & Yong L In vivo antitumour properties of tribenzyltin carboxylates in a 4T1 murine metastatic mammary tumour model: Enhanced efficacy by PLGA nanoparticles. *European Journal of Pharmaceutical Sciences* 2020, 142, 105140.
45. Pulaski BA & Ostrand-Rosenberg S Reduction of established spontaneous mammary carcinoma metastases following immunotherapy with major histocompatibility complex class II and B7.1 cell-based tumor vaccines. *Cancer Res* 1998, 58, 1486–1493. [PubMed: 9537252]
46. Yoneda T et al. Use of bisphosphonates for the treatment of bone metastasis in experimental animal models. *Cancer Treat Rev* 1999, 25, 293–299. [PubMed: 10544073]

47. Morecki S, Yacovlev E, Diab A & Slavin S Allogeneic cell therapy for a murine mammary carcinoma. *Cancer Res* 1998, 58, 3891–3895. [PubMed: 9731499]
48. Kau P et al. A mouse model for triple-negative breast cancer tumor-initiating cells (TNBC-TICs) exhibits similar aggressive phenotype to the human disease. *BMC Cancer* 2012, 12, 120. [PubMed: 22452810]
49. Yang L et al. Disease progression model of 4T1 metastatic breast cancer. *J Pharmacokinet Pharmacodyn* 2020, 47, 105–116. [PubMed: 31970615]
50. Tao K, Fang M, Alroy J & Gary GG Imagable 4T1 model for the study of late stage breast cancer. *BMC Cancer* 2008, 8, 1–19. [PubMed: 18173856]
51. Spiegel A et al. Neutrophils suppress intraluminal NK cell-mediated tumor cell clearance and enhance extravasation of disseminated carcinoma cells. *Cancer Discov* 2016, 6, 630–649. [PubMed: 27072748]
52. Snoderly HT, Boone BA & Bennewitz MF Neutrophil extracellular traps in breast cancer and beyond: Current perspectives on NET stimuli, thrombosis and metastasis, and clinical utility for diagnosis and treatment. *Breast Cancer Research* 2019, 21, 145. [PubMed: 31852512]
53. Kamioka Y, Takakura K, Sumiyama K & Matsuda M Intravital Förster resonance energy transfer imaging reveals osteopontin-mediated polymorphonuclear leukocyte activation by tumor cell emboli. *Cancer Sci* 2017, 108, 226–235. [PubMed: 27960041]
54. Yang C et al. Aged neutrophils form mitochondria-dependent vital NETs to promote breast cancer lung metastasis. *J Immunother Cancer* 2021, 9, e002875.
55. Mukai H et al. Pannexin1 channel-dependent secretome from apoptotic tumor cells shapes immune-escape microenvironment. *Biochem Biophys Res Commun* 2022, 628, 116–122. [PubMed: 36084549]
56. Snoderly HT, Boone BA & Bennewitz MF Neutrophil extracellular traps in breast cancer and beyond: Current perspectives on NET stimuli, thrombosis and metastasis, and clinical utility for diagnosis and treatment. *Breast Cancer Research* 2019, 21, 1–13. [PubMed: 30611295]
57. Monti M et al. Neutrophil extracellular traps as an adhesion substrate for different tumor cells expressing RGD-binding integrins. *Int J Mol Sci* 2018, 19, 2350. [PubMed: 30096958]
58. Kanamaru R et al. Neutrophil extracellular traps generated by low density neutrophils obtained from peritoneal lavage fluid mediate tumor cell growth and attachment. *Journal of Visualized Experiments* 2018, 138, 1–6.
59. Spiegel A et al. Neutrophils suppress intraluminal NK cell-mediated tumor cell clearance and enhance extravasation of disseminated carcinoma cells. *Cancer Discov* 2016, 6, 630–649. [PubMed: 27072748]
60. Romero AI, Thorén FB, Brune M & Hellstrand K NKp46 and NKG2D receptor expression in NK cells with CD56dim and CD56bright phenotype: Regulation by histamine and reactive oxygen species. *Br J Haematol* 2006, 132, 91–98. [PubMed: 16371024]
61. Mellqvist U-H et al. Natural killer cell dysfunction and apoptosis induced by chronic myelogenous leukemia cells: role of reactive oxygen species and regulation by histamine. *Blood* 2000, 96, 1961–1968. [PubMed: 10961901]
62. Bellner L et al. A Proinflammatory Peptide from Herpes Simplex Virus Type 2 Glycoprotein G Affects Neutrophil, Monocyte, and NK Cell Functions. *The Journal of Immunology* 2005, 174, 2235–2241. [PubMed: 15699157]
63. Chen Y et al. Nab-paclitaxel promotes the cancer-immunity cycle as a potential immunomodulator. *Am J Cancer Res* 2021, 11, 3445–3460. [PubMed: 34354854]
64. Lau TS et al. Paclitaxel induces immunogenic cell death in ovarian cancer via TLR4/IKK2/SNARE-dependent exocytosis. *Cancer Immunology Research* 2020, 8, 1099–1111. [PubMed: 32354736]
65. Sprooten J et al. Trial watch: chemotherapy-induced immunogenic cell death in oncology. *OncImmunology*, 2023, 12, 1703449.

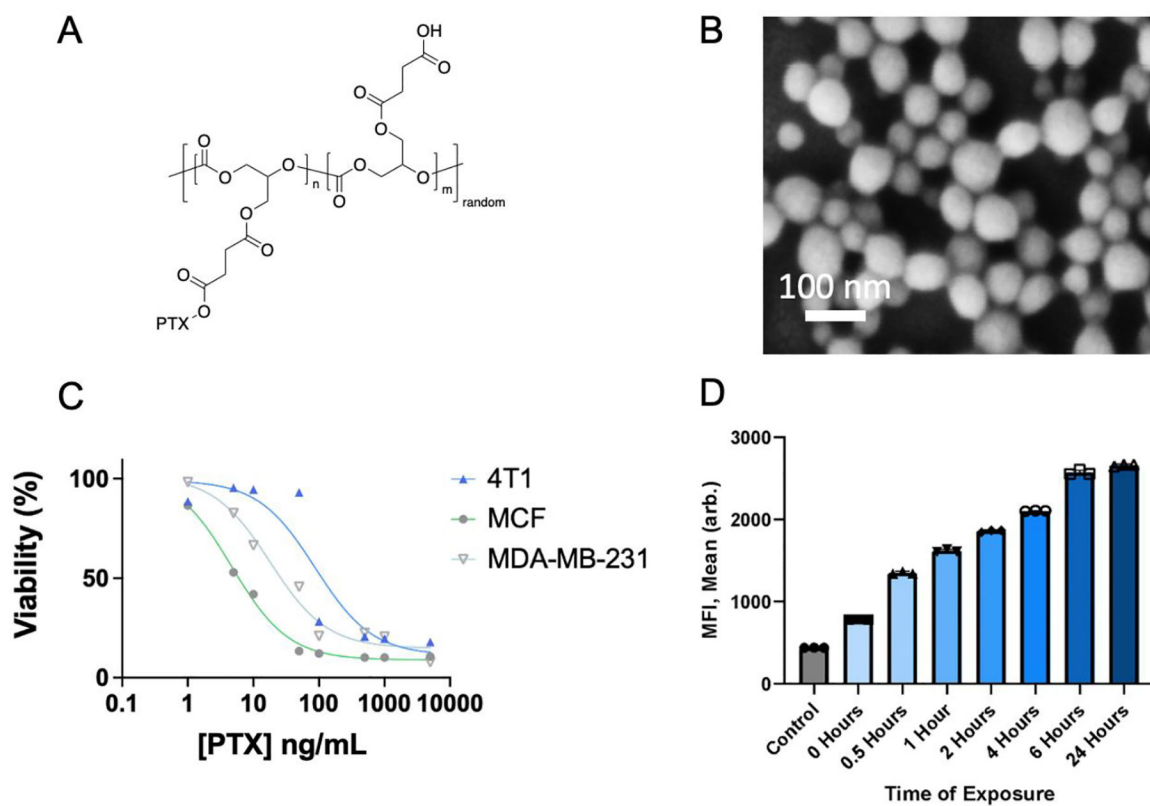


Figure 1. Chemical Structure of PGC-PTX (A). SEM micrograph of PGC-PTX + PTX NPs (B). In vitro characterization of PGC-PTX + PTX NP cytotoxicity against several breast cancer cell lines (C) and cellular uptake of rhodamine-conjugated NPs in 4T1 cancer cells, as determined by flow cytometry (D).

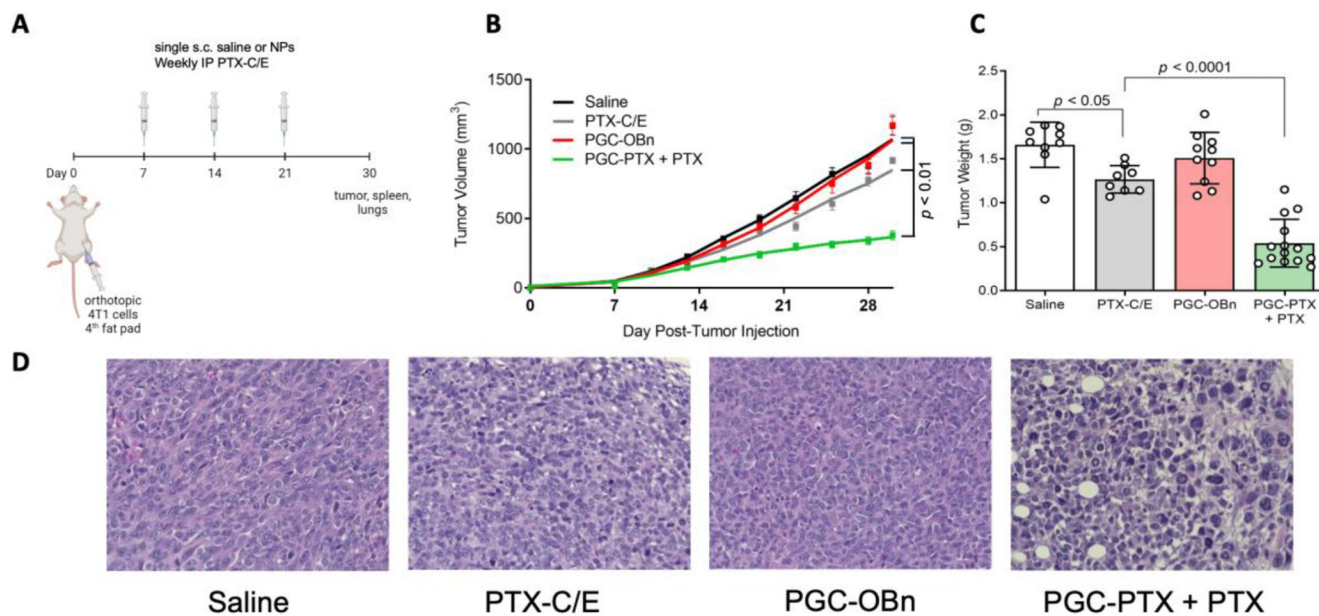


Figure 2. (A) Treatment scheme in 4T1 metastatic breast cancer murine model. (B) Tumor volume over time. (C) Primary tumor weight at day 30. (D) Histological evaluation via H&E staining of primary tumor at day 30 (40X magnification).

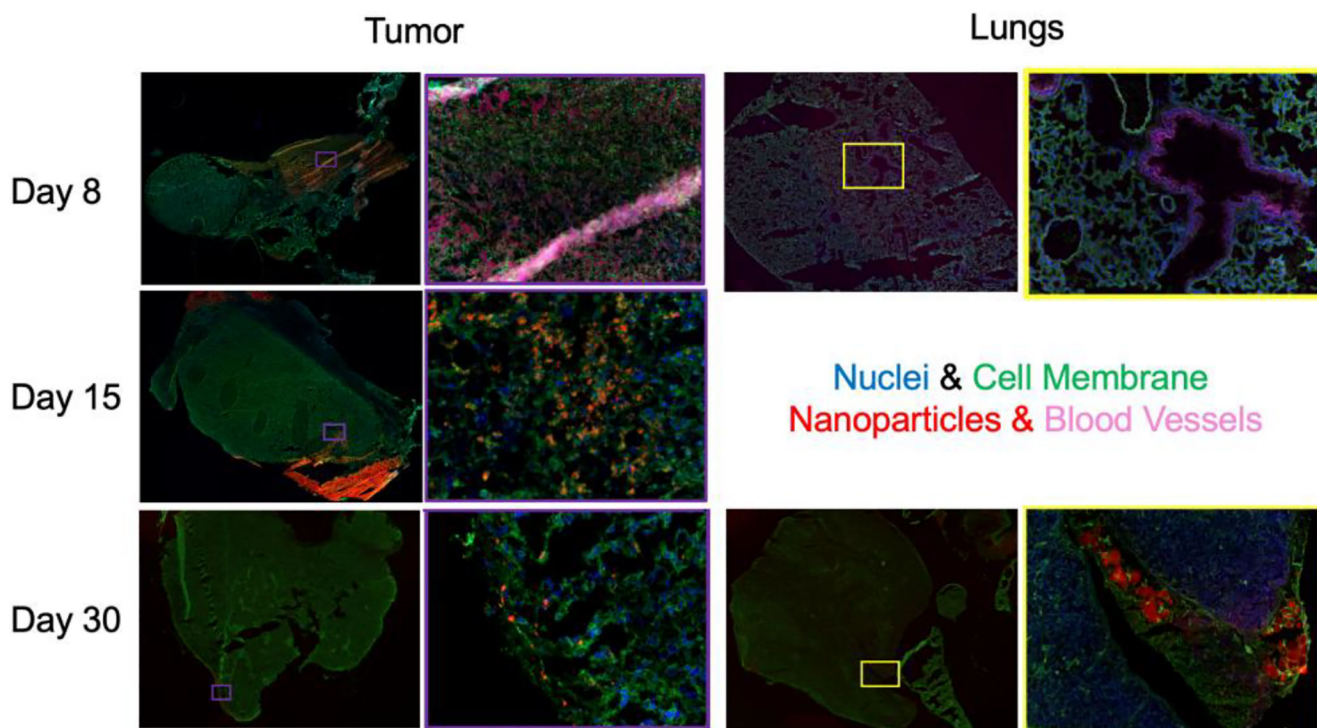


Figure 3. Representative fluorescent microscopy images at 20x (left) and 200x (right) of tumor and lungs as a function of time after PGC-PTX-Rho + PTX NP subcutaneous injection near the tumor.

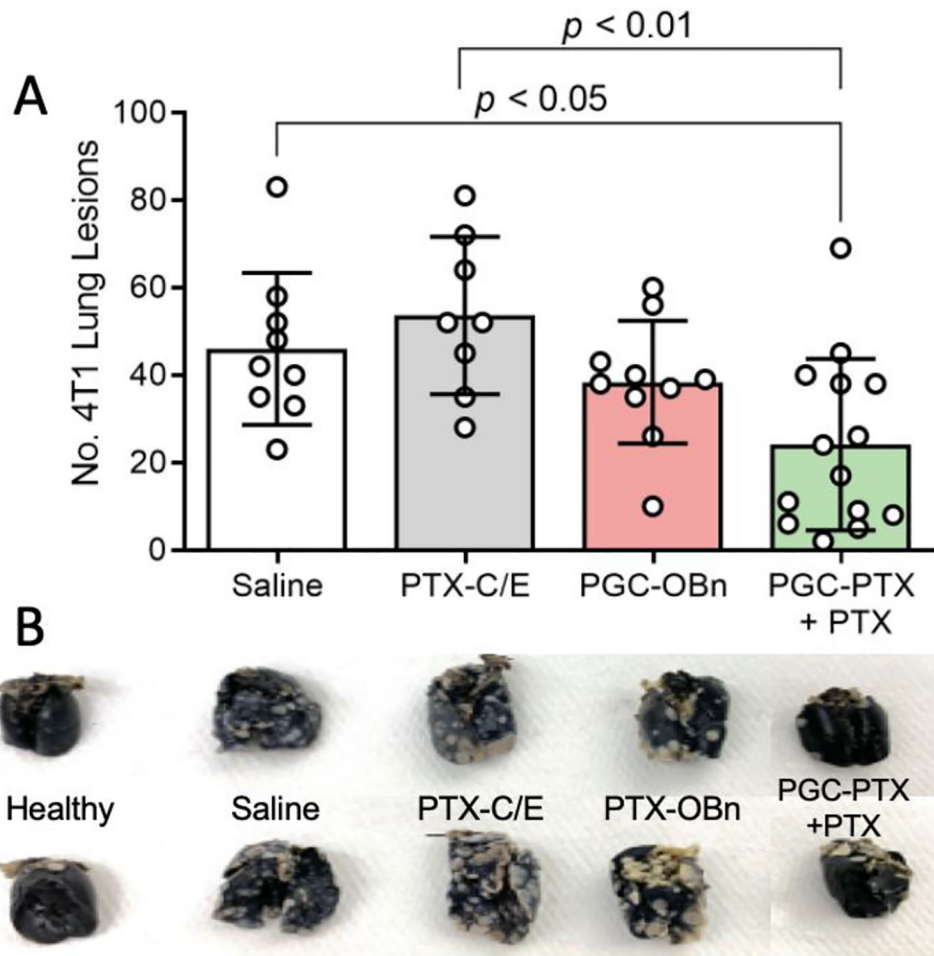


Figure 4. Number of metastatic lesions in lungs on day 30 post-treatment (A) with representative image for each group, compared to healthy control (B).

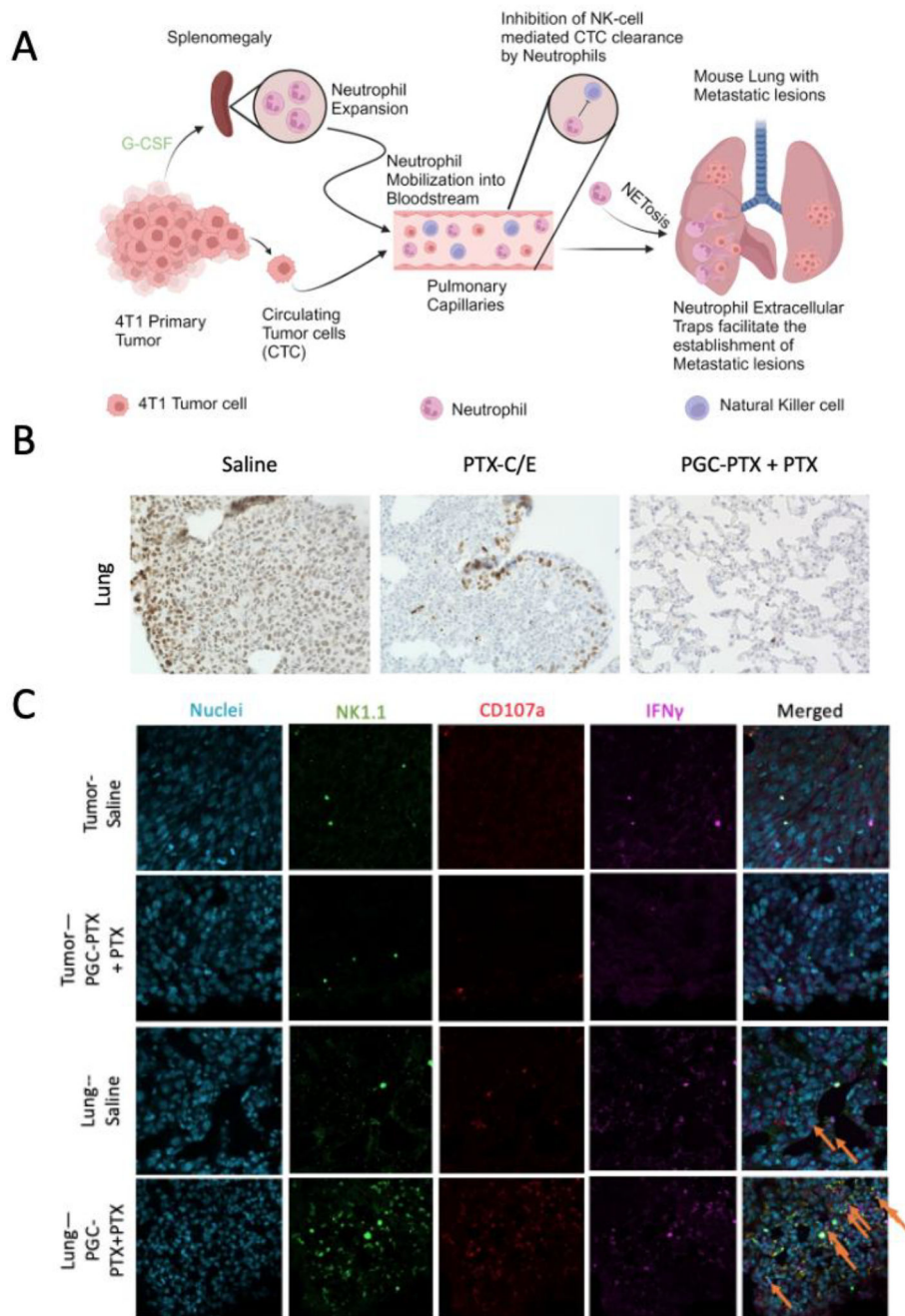


Figure 5. (A) Schematic of the pathway and mechanism establishing metastasis in the lung. Images after immunohistochemical staining of neutrophil extracellular traps (NETs) Created with [BioRender.com](https://www.biorender.com) (B) and activated NK cells (C) (40X magnification).